# Atypical phase behaviour of quinoa protein isolate in mixture with maltodextrin

Campos Assumpcao De Amarante, Marina; Maccalman, Thomas; Harding, Stephen E.; Spyropoulos, Fotis; Gras, Sally L; Wolf, Bettina

*DOI:*
10.1016/j.foodres.2022.112064

Food Research International 162 (2022) 112064

Contents lists available at ScienceDirect

Food Research International

journal homepage: www.elsevier.com/locate/foodres

# Atypical phase behaviour of quinoa protein isolate in mixture with maltodextrin

Marina Campos Assumpção de Amarante [a,c], Thomas MacCalman [b], Stephen E. Harding [b], Fotis Spyropoulos [a], Sally Gras [c], Bettina Wolf [a,*]

[a] School of Chemical Engineering, University of Birmingham, Edgbaston, Birmingham, West Midlands B15 2TT, United Kingdom
[b] National Centre for Macromolecular Hydrodynamics, School of Biosciences, University of Nottingham, Sutton Bonington Campus, Loughborough, Leicestershire LE12 5RD, United Kingdom
[c] Department of Chemical Engineering and Bio21 Molecular Science and Biotechnology Institute, The University of Melbourne, Parkville, Victoria 3010, Australia

ARTICLE INFO

*Keywords:*
Biopolymer mixture
Phase diagram
Depletion flocculation
Plant protein
Microstructure
Molecular weight distribution

ABSTRACT

Consumers are increasingly looking for new plant-based alternatives to substitute animal proteins in their diets but for some applications it can be difficult to achieve the desired product microstructure using only plant proteins. One approach to facilitate structuring is to mix these plant-based ingredients with a polysaccharide. Here, the phase behaviour and microstructure of quinoa protein isolate (QPI) in mixture with maltodextrin (MD) of two dextrose equivalents (DE 7 and 2) were investigated. The binodals of both QPI-MD phase diagrams showed an atypical shape, where the concentration of MD in the QPI-rich phase and of QPI in the MD-rich phase increased with overall biopolymer concentration. Molecular weight distribution and microstructure analyses revealed that both maltodextrins fractionated between the phases and were probably entrapped within the volume-spanning protein network in the QPI-rich phase, indicating a depletion flocculation mechanism of phase separation. The pre-heating of QPI and the removal of salt from the systems resulted in similarly atypical phase diagrams. The approach presented contributes to our understanding of the phase behaviour of mixtures between plant proteins and polysaccharides, while the results suggest that the formulation of plant-based products of predictable properties may be more challenging than anticipated.

## 1. Introduction

Biopolymer mixtures, mainly those composed of a protein and a polysaccharide, have been extensively applied in the creation of a wide range of microstructures in the food and healthcare industries. Polymer-polymer and polymer–solvent interactions influence the physicochemical properties of these mixtures, consequently defining their possible applications. The design of new products containing these systems relies on an understanding of the mechanism by which these components interact and the relationship between microstructure and product rheology (Frith, 2010).

Traditionally, studies on biopolymer mixtures have mainly focused on systems composed of polysaccharides and animal-based proteins, such as whey protein (Kim, Decker, & McClements, 2006), bovine serum albumin (Antonov & Wolf, 2006) and gelatine (Kasapis, Morris, Norton, & Clark, 1993). Over the last decade, though, the research community and industry have paid increasing attention to plant proteins due to consumer concerns with the sustainability of the animal protein industry (Mattice & Marangoni, 2019). At first, studies emerged on the phase behaviour of polysaccharides and isolated protein fractions of plant origin, i.e., globulin fraction or rubisco (Antonov, Losinskaya, Grinberg, Dianova, & Tolstoguzow, 1979; Antonov, Dmitrochenko, & Leontiev, 2006; Antonov & Soshinsky, 2000). More recently, protein mixtures (referred to as protein concentrate or isolate with no clear differentiation in terms of protein content in the mixtures among the publications cited further on) containing more than one isolated plant protein, have been progressively explored. Soy and pea protein appear to be the most studied plant proteins for the creation of biopolymer mixtures with polysaccharides, although very few studies on phase behaviour can be found (Li, Hua, Qiu, Yang, & Cui, 2008a; Mession, Assifaoui, Cayot, & Saurel, 2012a; Mession, Assifaoui, Lafarge, Saurel, & Cayot, 2012b), where the majority focuses on the association between the biopolymers (Gharsallaoui, Yamauchi, Chambin, Cases, & Saurel, 2010; Guo, Su, Yuan, Mao, & Gao, 2019; Lan, Chen, & Rao, 2018; Lan, Ohm, Chen, &

* Corresponding author.
*E-mail address:* b.wolf@bham.ac.uk (B. Wolf).

https://doi.org/10.1016/j.foodres.2022.112064
Received 27 June 2022; Received in revised form 14 October 2022; Accepted 16 October 2022
Available online 20 October 2022

Rao, 2020b, 2020a).

Quinoa (*Chenopodium quinoa* Willd.) is considered an attractive non-animal protein source due to its high nutritional value and absence of gluten (Föste, Elgeti, Brunner, Jekle, & Becker, 2015). Its global consumption has recently become very popular, and its production expanded from the traditional Andes region of South America to a wide range of different cultivation areas worldwide (Murphy, Matanguihan, Fuentes, Gómez-Pando, Jellen, Maughan, & Jarvis, 2019). Quinoa protein isolate (QPI) is a protein mixture prepared via a fractionation process from quinoa, and has been increasingly investigated in the last few years, especially due to its complete essential amino acid profile (Cerdán-Leal, López-Alarcón, Ortiz-Basurto, Luna-Solano, & Jiménez-Fernández, 2020; Mir, Riar, & Singh, 2019; Steffolani, Villacorta, Morales-Soriano, Repo-Carrasco, León, & Pérez, 2016), which meets the amino acid requirements for adults suggested by the Food and Agriculture Organization of the United Nations (FAO), the World Health Organization (WHO) and the United Nations University (UNU) (Vilcacundo & Hernández-Ledesma, 2017; WHO/FAO/UNU, 2007). QPI has been shown to present a range of potential applications in the food industry due to its functional properties, which are largely affected by extraction pH, including thermal stability and gel formation (Abugoch, Romero, Tapia, Silva, & Rivera, 2008; Ruiz, Xiao, van Boekel, Minor, & Stieger, 2016a). However, to the best of the authors' knowledge, there are no studies on the phase behaviour of QPI in mixture with polysaccharides aiming at the design of microstructures for food applications.

Maltodextrin (MD) is a polysaccharide derived from the acidic or enzymatic hydrolysis of starch (Saavedra-Leos, Leyva-Porras, Araujo-Díaz, Toxqui-Terán, & Borrás-Enríquez, 2015). Its chemical structure consists of D-glucose monomers linearly linked by α-1,4 glucosidic bonds (Klinjapo & Krasaekoopt, 2018; Zheng, Jin, & Zhang, 2007) and it may contain branch points arising from α-1,6 bonds (Chronakis, 1998). Maltodextrins are characterised by their dextrose equivalent (DE), which refers to the extent of starch hydrolysis and represents the percentage of reducing sugars, i.e., free glucose groups that define the reducing power of starch-derived polysaccharides (Wang & Wang, 2000). Generally, the higher the DE value, the greater the extent of starch hydrolysis and the lower the number-average molecular weight (Saavedra-Leos et al., 2015). The general properties of MD include low sweetness, the absence of odour and moderate viscosity and solubility in cold water. Therefore, maltodextrins are widely applied in the food industry to confer texture and bulk, or to replace fat in food products, as well as to assist in the spray-drying of flavours and seasonings (Wang & Wang, 2000; Zheng et al., 2007). The use of MD as a phase separating polysaccharide has been widely explored, mainly in a mixture with refined animal proteins, such as gelatine and caseinate (Beldengrün, Aragon, Prazeres, Montalvo, Miras, & Esquena, 2018; Kasapis et al., 1993; Loret, Schumm, Pudney, Frith, & Fryer, 2005; Manoj, Kasapis, & Chronakis, 1996; Williams, Fabri, Hubbard, Lundin, Foster, Clark, Norton, Lorén, & Hermansson, 2001). There is limited information, however, on the phase-separating behaviour of mixtures of MD and plant proteins (Nguyen, Lafarge, Murat, Mession, Cayot, & Saurel, 2014).

The aim of this study was to investigate the relationship between the phase behaviour of QPI and MD and the microstructure of these systems, envisaging the creation of tailored microstructures for the design of plant protein-enriched products. MD is a neutral polysaccharide and QPI has a negative net charge above its isoelectric point, i.e., pH 4.5 (Mir et al., 2019). Thus, aqueous mixtures of QPI and MD should be expected to separate into co-existing QPI- and MD-rich phases at pH 7.0, also known as segregative phase behaviour. Phase diagrams were constructed to represent the segregative phase behaviour of the mixtures, where a binodal curve separates the one- and two-phase regions, located below and above the curve, respectively. Parallel tie-lines connect the binodal points corresponding to the compositions of the co-existing phases (top and bottom) with the initial mixture composition (Dickinson, 2019).

In this study, the phase behaviour of QPI was investigated in mixture with maltodextrins of two different DE values, DE 2 and 7, i.e., different molecular weights, since the molecular weight of the polysaccharide is a key factor influencing the incompatibility of biopolymer mixtures (Tolstoguzov, 2000b). Molecular weight distributions of the MDs and micrographs of the separated phases were acquired in aid of understanding the observed phase behaviour. Additionally, the partial denaturation through heat treatment has been previously shown to affect the phase behaviour of other proteins (Chun, Hong, Surassmo, Weiss, Min, & Choi, 2014; Kim et al., 2006). Therefore, the influence of heat pretreatment on the phase diagram of QPI and MD of DE 2 was also investigated, as MD of DE 2 has been reported to show segregative phase behaviour with other proteins (Beldengrün et al., 2018; Manoj et al., 1996). Moreover, ionic strength affects protein structure and protein-polysaccharide interactions, consequently influencing the phase behaviour of the mixtures. Thus, the absence of salt in the QPI-MD systems was also studied in order to build a better understanding of these mixtures.

## 2. Materials and methods

### 2.1. Materials

The quinoa flour, produced from white quinoa seeds, was purchased from The British Quinoa Company® (Ellesmere, UK). According to the manufacturer, the flour contained, on a dry weight basis, 14.3 % protein, 65.7 % carbohydrate (of which 2.6 % was sugar), 6.8 % fat and 6.8 % fibre. Maltodextrin (MD) with a dextrose equivalent (DE) of 7 produced from corn starch (C*Dry MD) was purchased from Cargill® (USA). MD of DE 2 produced from potato starch (Paselli SA-2) was purchased from Avebe® (Netherlands). NaOH pellets (≥97 %) and NaCl (≥99.5 %) were purchased from Fisher Scientific® (UK). HCl (≥32 %) was purchased from Honeywell® (UK). Sodium azide (≥99.5 %) and starch assay kit were purchased from Sigma-Aldrich® (UK). Double distilled water with a resistivity of 15.0 MΩ.cm (Millipore®, UK) was used in all experiments.

### 2.2. Quinoa protein isolate extraction and characterisation

#### 2.2.1. Extraction from quinoa flour

Quinoa protein isolate was extracted from quinoa flour using the method of Ruiz et al. (2016a), except that the flour defatting step was omitted to avoid the use of organic solvents and the centrifugal speed was modified. Briefly, the flour was sieved through a 250 μm aperture sieve and suspended in water (10 %, w/w). The pH was adjusted to 9.0 using 1 M NaOH and the suspension was agitated at 22 °C for 4 h, then stored at 4 °C for 16 h. Afterwards, the suspension was centrifuged for 30 min at 10 °C and 8228 × g and the supernatant poured through a cheesecloth to separate the cream layer (Geerts, Dekkers, van der Padt, & van der Goot, 2018). The precipitate and cream layer were discarded. The pH of the supernatant was adjusted to 4.5 using 1 M HCl to induce isoelectric precipitation of the protein, followed by centrifugation as described above. The precipitate was rinsed by re-suspending in distilled water and centrifuged once more. Finally, the precipitate was re-suspended in distilled water, neutralised using 1 M NaOH and freeze-dried for 72 h (Labogene®, Scanvac Coolsafe, Denmark). The lyophilised quinoa protein isolate (QPI) was kept at 4 °C until use.

#### 2.2.2. Compositional analysis and protein yield

The total protein content of the prepared QPI and quinoa flour was determined as total nitrogen content, via elemental analysis (Thermo Flash EA 1112, ThermoFisher Scientific®, UK), and converted to total protein using a conversion factor of 5.85 (Abugoch et al., 2008; Ruiz et al., 2016a). Moisture, ash, and fat were assayed through methods from the Association of Official Analytical Chemists (AOAC, 2002), i.e.,

method numbers 934.01, 923.03, and 920.39 (using hexane as solvent), respectively. Carbohydrate content was determined by difference. Starch content was determined using a starch assay kit (Supelco™ Analytical, Sigma Aldrich® , USA), where starch is hydrolysed to glucose by amyloglucosidase and glucose concentration measured by the change in absorbance at 340 nm.

Protein yield was calculated considering the total protein content of QPI and of quinoa flour, using Eq. (1).

$$Protein\ yield(\%) = \frac{total\ protein\ content\ QPI\ (\%) \times QPI\ weight\ (g)}{total\ protein\ content\ quinoa\ flour\ (\%) \times flour\ weight\ (g)} \times 100\% \quad (1)$$

### 2.3. Acquisition of phase diagrams

For the acquisition of QPI-MD phase diagrams, stock solutions of both polymers were prepared in 0.1 M NaCl solution, as salt promotes phase separation (Grinberg & Tolstoguzov, 1997), and mixed at different ratios. The QPI-MD mixtures were then centrifuged to obtain two phases and the biopolymer composition in each phase was determined to construct phase diagrams. Mathematical approximations of the phase diagrams were also undertaken.

#### 2.3.1. Preparation of stock solutions

A QPI stock solution (10 %, w/w) was prepared by dissolving the lyophilised QPI in 0.1 M NaCl containing 0.03 % (w/w) sodium azide to prevent microbial growth. The solution was stirred constantly for 2 h at pH 9.0 (adjusted with 1 M NaOH). The pH was adjusted to 7.0 (with 1 M HCl) and the stock solution was kept stirring overnight on a magnetic stirrer at 22 °C. To remove any insoluble material, the QPI stock solution was centrifuged for 1 h at 10 °C and 2400 × g and used immediately.

Stock solutions of maltodextrin of DE 7 and DE 2 were prepared by dissolving the powders in 0.1 M NaCl (containing 0.03 % (w/w) sodium azide) at 90 °C under constant stirring. After the powders appeared to be completely dissolved, the solutions were cooled to room temperature (22 °C) and used immediately after pH adjustment to 7.0 using 1 M NaOH.

#### 2.3.2. Preparation of phase-separated QPI and MD mixtures

Mixtures (10 g) of QPI and MD of DE 7 and 2, respectively, containing different concentrations of both polymers were prepared by mixing weighted amounts of QPI and MD stock solutions with 0.1 M NaCl (containing 0.03 % (w/w) sodium azide). Four mixtures of each system were studied, in concentration ranges of 0.2 – 4.3 % QPI (w/w) and 0.4 – 5.7 % MD (w/w). The mixtures were stirred for 2 h at 22 °C, then transferred to graduated centrifuge tubes and kept for approximately 16 h at 22 °C to allow for phase separation. The mixtures were then centrifuged for 1 h at 10 °C and 2400 × g and the equilibrium phases were separated with a pipette.

#### 2.3.3. Experimentally determined phase diagrams

Phase volume fractions were determined using a graduated cylinder and phase densities were calculated from the weight of samples of known volume to obtain the phase compositions in w/w. QPI concentration (x-axis of phase diagrams) was determined by measurement at 280 nm using an UV–vis spectrophotometer (Orion AquaMate 8000, Thermo-Scientific® , UK), utilising solutions of known concentrations of lyophilised QPI for the calibration curve. Maltodextrin concentration (y-axis of phase diagrams) was determined in each phase by the sulfuric acid-UV method (Albalasmeh, Berhe, & Ghezzehei, 2013), used for the determination of monosaccharides, disaccharides and polysaccharides of high molecular weight. Briefly, 1 mL of sample was acidified with 3 mL of concentrated sulfuric acid, then agitated in a vortex for 30 s and cooled to room temperature (22 °C) in an ice bath before measuring the absorption of the samples using an UV–vis spectrophotometer at 315 nm. MD concentrations were calculated from calibration curves acquired for each MD.

Finally, the experimental phase diagrams were constructed by plotting the tie-lines and manually fitting the binodals to the equilibrium phases points. The phase separation threshold corresponds to the minimum overall biopolymer concentration in the mixture required for phase separation (Tolstoguzov, 2002) and it was calculated as the point of contact between a tangent line with a slope of −1 that crosses equal segments of both axes and the binodal (Antonov, Lashko, Glotova, Malovikova, & Markovich, 1996). The critical point gives the composition of the system that demixes into phases of the same volume and composition and it was calculated as the point of interception of the binodal with the rectilinear diameter, i.e., a straight line that connects the composition of the system at the centre of each tie-line, i.e., at 50:50 phase volume (Tolstoguzov, 2002). The critical point and threshold point are unique characteristics of a phase diagram and if they coincide, the phase diagram is symmetrical. On the other hand, as the distance between the critical and threshold points increases, the phase diagram becomes increasingly asymmetrical (Zaslavsky, 1995). Several mixtures of each experimental phase diagram were prepared and analysed twice to verify reproducibility.

#### 2.3.4. Mathematical approximations of the phase diagrams

The phase diagrams were also mathematically approximated, using the volume fraction method suggested by Spyropoulos, Portsch, & Norton (2010). The method consists of the determination of the approximate composition of the equilibrium phases of a given aqueous two-phase system (ATPS) using the initial concentration of both biopolymers in the mixture and the volume fraction of each phase after phase separation. The following assumptions were made: (1) both biopolymers are pure and consist of one species of constant molecular weight, (2) the mixtures display classical segregative phase separation behaviour, and (3) the tie-lines of the phase diagrams are parallel, i.e., of the same slope (STL).

A two-parameter exponential decay function (Eq. (2)) was fitted to the top and bottom phases concentration data to give the binodals of the phase diagrams.

$$[MD] = a \times e^{-b \times [QPI]} \quad (2)$$

where [MD] and [QPI] correspond to the concentration of MD and QPI, respectively, and $a$ and $b$ are best fit parameters that describe the shape of the binodal. Tie-lines were calculated using Equations (3a-c):

$$[MD]_I = [MD]^0 + STL \times [QPI]_I \quad (3a)$$

$$[MD]_T = [MD]^0 + STL \times [QPI]_T \quad (3b)$$

$$[MD]_B = [MD]^0 + STL \times [QPI]_B \quad (3c)$$

where subscripts I, T and B relate to the initial mixture, the top and bottom phase after phase separation, respectively. $[MD]^0$ corresponds to the intercept between the y-axis of the phase diagram and the tie-line, and STL corresponds to the slope of the tie-line. Combining Equations (3a), (3b) and (3c), and consequently eliminating $[MD]^0$ and STL, gives Eq. (4):

$$\frac{[MD]_T - [MD]_I}{[MD]_B - [MD]_I} = \frac{[QPI]_T - [QPI]_I}{[QPI]_B - [QPI]_I} \quad (4)$$

The compositions of the top and bottom phases must lie on the binodal described by Eq. (2). For maltodextrin this concentration is:

$$[MD]_T = a \times e^{-b \times [QPI]_T} \quad (5a)$$

$$[MD]_B = a \times e^{-b \times [QPI]_B} \quad (5b)$$

Finally, each tie-line is divided into two segments: $\overline{TI}$ and $\overline{BI}$, where I, T and B correspond to the initial, top and bottom phase composition,

respectively. As pointed out by Spyropoulos et al. (2010), Zaslavsky (1995) has shown that the ratio between the length of each of these segments and the length of the entire tie-line $\overline{TB}$ corresponds to the volume fraction of the top ($Vf_T$) and bottom ($Vf_B$) phases at equilibrium:

$$Vf_T = \frac{\overline{TI}}{\overline{TB}} = \frac{[QPI]_I - [QPI]_B}{[QPI]_B - [QPI]_T} \tag{6a}$$

$$Vf_B = \frac{\overline{BI}}{\overline{TB}} = \frac{[QPI]_I - [QPI]_T}{[QPI]_B - [QPI]_T} \tag{6b}$$

Therefore, the QPI and MD concentrations in the top and bottom phases ($[QPI]_T$, $[QPI]_B$, $[MD]_T$, $[MD]_B$) can be calculated based on the initial biopolymer concentration in the mixtures and the experimentally determined volume fractions of the top and bottom phases after phase separation, by numerically solving Equations (4), 5a (or 5b) and 6a (or 6b). Fitting Equation (2) to the resulting data set then allows the determination of the binodal. The phase separation thresholds and the critical points for the mathematical approximations were determined as described for the experimentally determined phase diagrams (2.3.3).

### 2.4. Microstructure visualisation

The microstructure of initial mixtures and equilibrium phases was visualised at 22 °C using an optical microscope (DM 2500 LED, Leica® , CH) in phase contrast mode (Sarbon, Badii, & Howell, 2015). A droplet of sample was added to each slide (not diluted) and covered with a cover slip.

### 2.5. Determination of molecular weight distribution of MD

The molecular weight distribution of both MD samples was determined by size exclusion chromatography coupled with multi angle laser light scattering (*SEC*-MALS), consisting of a Postnova Analytics® PN7505 degassing unit (Germany), a Shimadzu® LC-10 AD HPLC Pump (UK), a Spark-Holland® Marathon Basic autosampler (Netherlands), a Shodex™ LB-G 6B guard column (USA) and a Shodex™ LB-805 column (USA) connected in series. Light scattering intensities were measured simultaneously at 18 angles as a function of elution volume using a DAWN® HELEOS™ II light scattering photometer, connected in series to a ViscoStar® II on-line differential viscometer and an Optilab® rEX refractive index detector (Wyatt Technology Corporation, USA). Samples were filtered using 0.2 μm polyvinylidene difluoride (PVDF) Whatman® Puradisc 25 syringe filters. Aliquots of 50 μL of each MD stock solution were injected onto the columns at 22 °C. The eluent used was 0.1 M NaCl with 0.01 % ProClin™ 150 (Sigma-Aldrich®) at a flow rate of 0.5 mL/min. The laser was used at a wavelength of 633 nm and the refractive increment for maltodextrin was 0.155 mL/g. ASTRA™ (Version 6) software was used to calculate the weight average molecular weight ($M_w$). Thermodynamic non-ideality effects were assumed to be negligible, due to low sample concentrations and their constant dilution in the columns (Horton, Harding, & Mitchell, 1991).

### 2.6. Differential scanning calorimetry

The thermal properties of QPI were determined by differential scanning calorimetry (DSC; μDSC3evo run, Setaram Instrumentation® , France). QPI (10 %, w/w) was suspended in distilled water and kept under magnetic stirring for 1 h at 22 °C, without pH adjustment. Hermetically sealed pans were filled with around 0.5 g of QPI suspensions. A hermetically sealed pan with a matching mass of distilled water was used as reference. Samples were heated at a rate of 2 °C/min from 20 to 120 °C, kept at this temperature for 5 min and then cooled at the same rate to 20 °C. The denaturation temperature ($T_d$), defined as the temperature where the maximum transition peak occurred, and the denaturation enthalpy (ΔH), defined as the area below the transition peak, were calculated using the CALISTO software (Seteram Instrumentation® , France). Enthalpy was then converted to J/g QPI by considering the sample concentration (10 %, w/w).

### 2.7. Effect of heat pre-treatment and absence of salt on phase behaviour

The effect of protein heat pre-treatment and absence of salt on the phase behaviour were also investigated. Both factors can affect both protein structure and protein-polysaccharide interactions, thus influencing phase behaviour. For the study of heat pre-treatment, the QPI stock solution was incubated at 55 °C for 30 min and then cooled to room temperature (HTQPI). For the investigation of the effect of salt, both QPI and MD stock solutions were prepared as described in 2.3.1, except for the absence of NaCl. Phase diagrams were then acquired as outlined in 2.3.3.

## 3. Results and discussion

### 3.1. Composition and yield of QPI

The total protein content of the quinoa flour used here was of 15.2 %, close to previous reports of 14.0 % protein in quinoa seeds (Elsohaimy, Refaay, & Zaytoun, 2015). QPI was extracted by an aqueous-based extraction protocol at pH 9.0 followed by precipitation at pH 4.5, resulting in a protein yield of 19.4 % and a wet weight protein content (i.e., purity) of 59 ± 3 %. Both values are within the wide range previously reported in literature for QPI extracted at pH 9.0: ~9.2–37 % for protein yield (Nongonierma, Le Maux, Dubrulle, Barre, & FitzGerald, 2015; Ruiz, Opazo-Navarrete, Meurs, Minor, Sala, van Boekel, Stieger, & Janssen, 2016b) and ~ 41–96 % for protein content (Mir et al., 2019; Nongonierma et al., 2015; Ruiz et al., 2016b; Ruiz et al., 2016a; Steffolani et al., 2016). The differences between protein extraction yield and content arise from variations in extraction protocols and the use of different quinoa cultivars. For example, the protein content obtained for QPI extracted at pH 9.0 from six different quinoa varieties varied between ~ 85–96 % (Steffolani et al., 2016). The QPI extracted here further contained 11 ± 3 % fat, 3.0 ± 0.6 % starch, 1.4 ± 0.8 % moisture, 3.0 ± 0.5 % ash and 25.6 % carbohydrate calculated by difference. The fat content of QPI is usually not reported in literature, presumably because it is non-detectable. However, most studies apply a quinoa flour defatting step using hexane or petroleum ether prior to QPI extraction. Yang, de Campo, Gilbert, Knott, Cheng, Storer, Lin, Luo, Patole, & Hemar (2022) reported a 4.9 % fat content for their QPI extracted from defatted quinoa flour. Here, aqueous fractionation was used without prior flour defatting to avoid the use of toxic organic solvents. Therefore, a fraction (8.2 %) of the fat contained in the flour was carried over into the QPI extract.

### 3.2. QPI-MD phase separation behaviour

The key aim of this study was to elucidate the phase behaviour of QPI and maltodextrin of DE 7 and DE 2 in aqueous mixture, and thus phase diagrams were constructed. Molecular weight data and micrographs were additionally acquired as supportive evidence for the assumed type of phase behaviour displayed by the QPI-MD systems. Fig. 1 shows the mathematical approximation of the phase behaviour assuming segregative phase separation into two aqueous phases, each enriched in one of the two biopolymers. The experimentally acquired phase diagrams are shown in Fig. 2. The QPI concentration axis in the phase diagrams refers to UV–vis spectrophotometer measurements reported in 2.3.3. Alternative representations of the phase diagrams based on total protein are included in Supplementary material – A.

The mathematical approximation method (Fig. 1) suggests that QPI is less compatible with MD of DE 7 than with MD of DE 2, evidenced by the lower phase separation threshold value of 2.5 % for QPI-MD DE 7, as opposed to 4 % for QPI-MD DE 2. Since the phase separation threshold

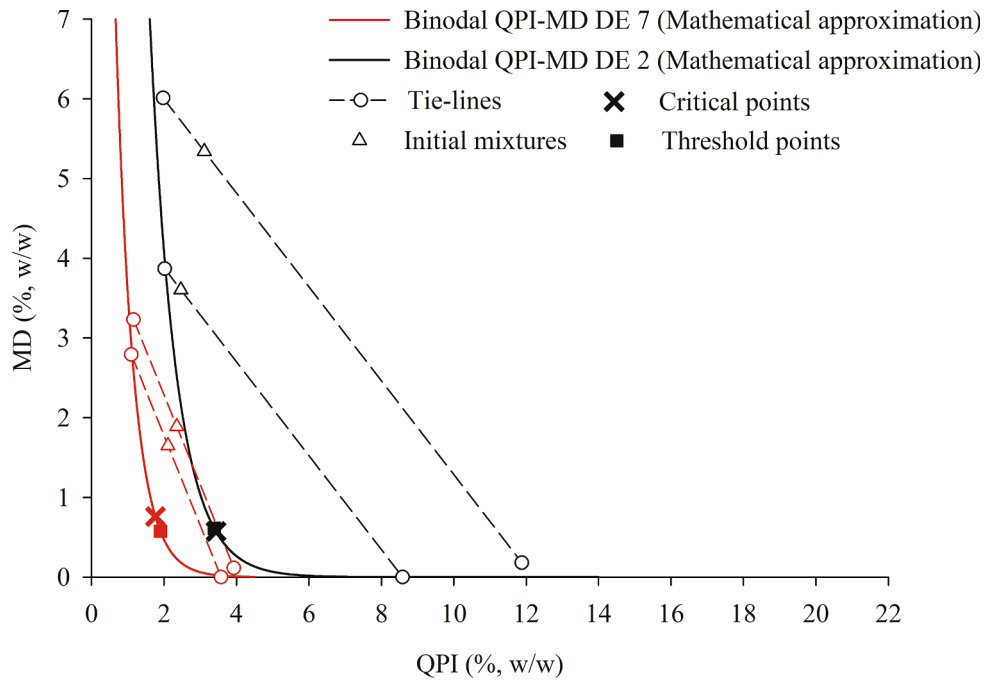


**Fig. 1.** Mathematical approximations of the phase diagrams between QPI and MD of DE 7 or DE 2 at pH 7.0, 22 °C and 0.1 M NaCl.

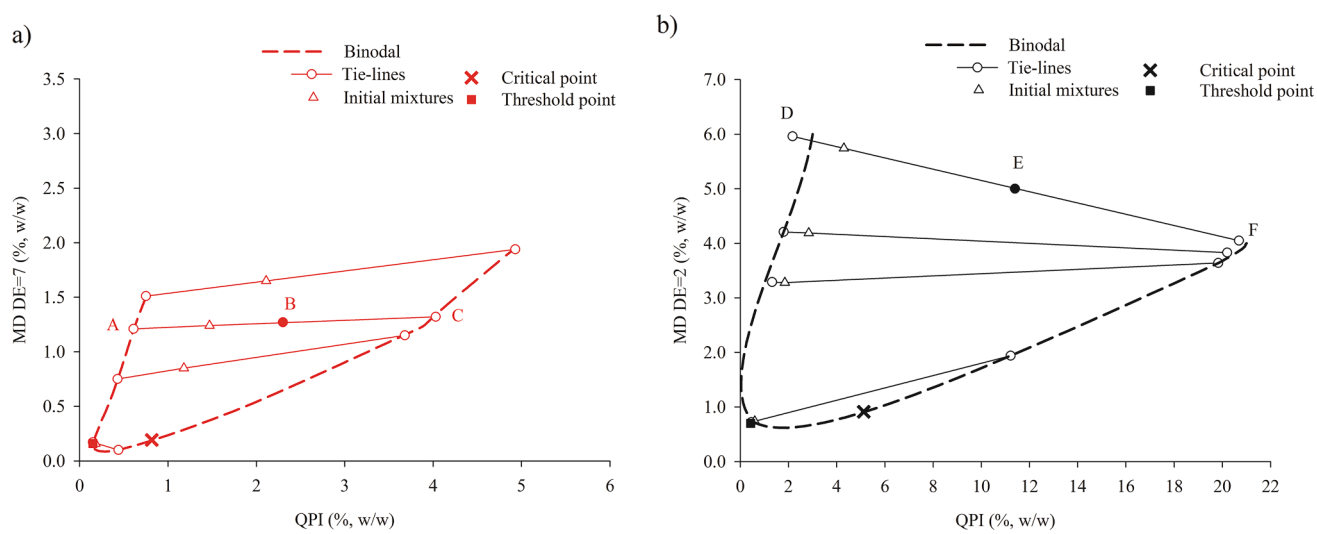


**Fig. 2.** Experimental phase diagrams between QPI and MD DE 7 or DE 2 at pH 7.0, 22 °C and 0.1 M NaCl: a) QPI-MD DE 7 and b) QPI-MD DE 2. The letters identify samples that were imaged. The standard error (SE) for polymer concentrations in either phase of the QPI-MD DE 7 mixtures ranged between 0.1 and 1.0 %, resulting in coefficients of variation (CV = SE/mean) of less than 20 %. The SE for the QPI-MD DE 2 mixtures ranged between 0.05 and 1.8 %, resulting in CVs of less than 10 %, except for one outlier of 31 % for MD concentration in one of the bottom phases.

corresponds to the minimum overall biopolymer concentration in the mixture required for phase separation (Tolstoguzov, 2002), a lower threshold value indicates a smaller area of miscibility, i.e., lower compatibility. The critical and threshold points are very close together for both systems, as demonstrated in Fig. 1, which indicates a good symmetry of the mathematical approximations.

The shape of both experimentally determined binodals is unusual, as it shows a shift away from both axes of the phase diagram, unlike the mathematically approximated binodals (Fig. 1). The shift is congruent with an increase in concentration of MD and QPI, respectively, in the QPI- and MD-rich phases with increasing overall biopolymer concentration in the system. This unusual behaviour may be due to molecular weight ($M_w$) fractionation of MD between the separated phases. Paselli SA2, the commercially available MD of DE 2 used here, has been reported to have a broad molecular weight distribution, and to fractionate between the separated phases when mixed with agarose above the phase separation threshold (Loret et al., 2005). Molecular weight fractionation between separated phases was also observed for other biopolymer mixtures, e.g., dextran-locust bean gum (Garnier, Schorsch, & Doublier, 1995), poly(ethylene oxide)-dextran (Edelman, van der Linden, & Tromp, 2003) and gelatin-dextran systems (Edelman, Tromp, & van der Linden, 2003). It is worth noting though that for all of the cited systems, including the agarose-Paselli SA2, classical segregative phase separation behaviour was reported.

To ascertain whether molecular weight fractionation caused the behaviour observed here, the $M_w$ distribution of both MDs was assessed. The results of the *SEC*-MALS analysis of the maltodextrins and of the bottom phases of the QPI-MD mixtures are depicted in Fig. 3. MD of DE 7

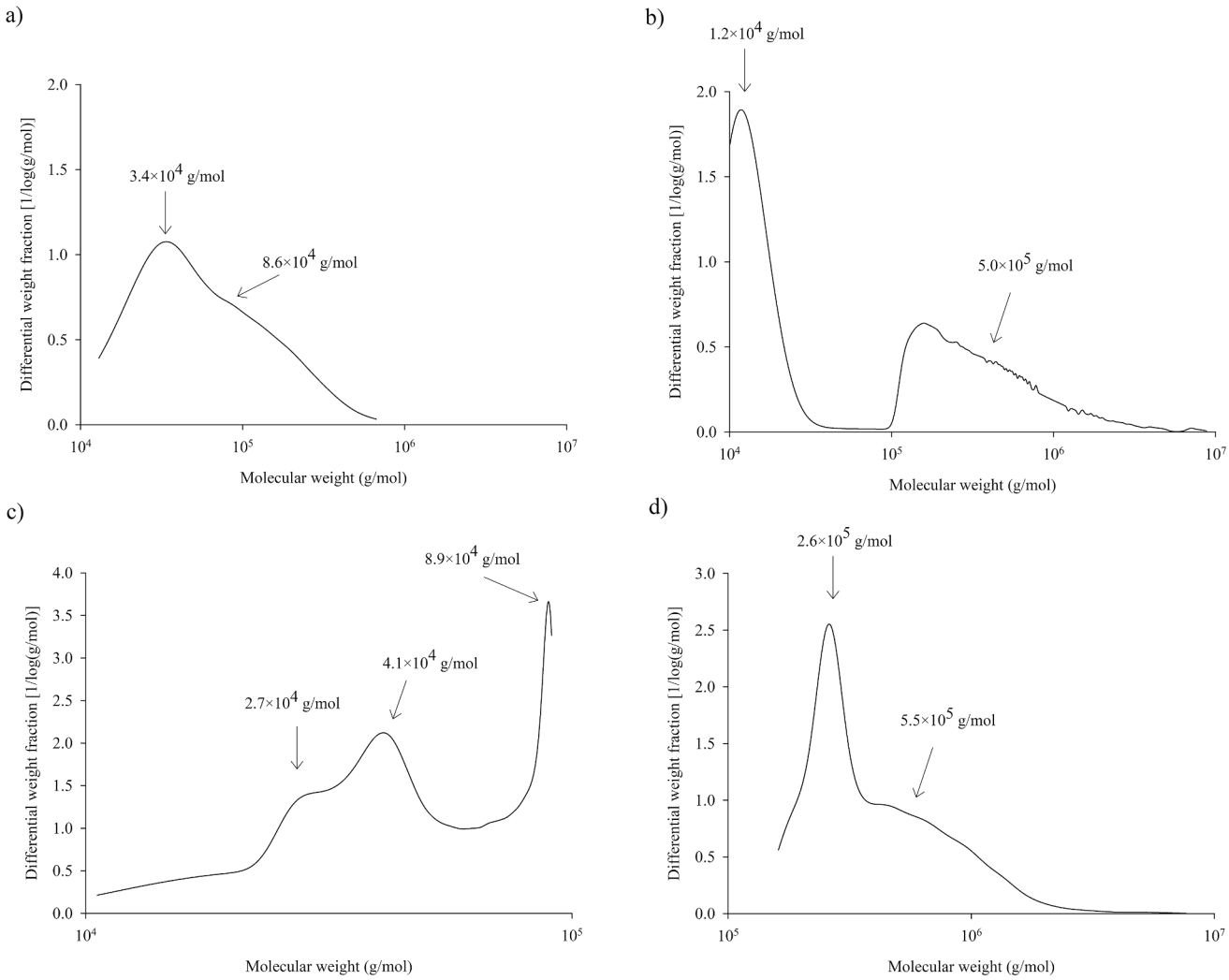


**Fig. 3.** Molecular weight distribution of a) MD of DE 7 and b) MD of DE 2, and of the bottom phases of mixtures c) 4.9 % QPI + 1.9 % MD DE 7 and d) 20.7 % QPI + 4 % MD DE 2 in 0.1 M NaCl at 22 °C.

showed a single peak at $3.4 \times 10^4$ g/mol, with a shoulder at $8.6 \times 10^4$ g/mol (Fig. 3a). In contrast, MD of DE 2 had a broad molecular weight distribution with two main peaks at ~ $1.2 \times 10^4$ g/mol and ~ $5 \times 10^5$ g/mol (Fig. 3b), in agreement with Loret et al. (2005).

The *SEC*-MALS data suggests that both MDs fractionated between the phases, based on the chromatograms for the bottom phases of the mixtures (Fig. 3c-d). The chromatogram for the bottom phase of the QPI-MD DE 7 mixture, which consisted of 4.9 % QPI and 1.9 % MD DE 7 shown in Fig. 3c has two peaks: one at $4.1 \times 10^4$ g/mol, with a shoulder at $2.7 \times 10^4$ g/mol, and another one at $8.9 \times 10^4$ g/mol. Based on published literature (Abugoch et al., 2008; Kaspchak, Oliveira, Simas, Franco, Silveira, Mafra, & Igarashi-Mafra, 2017; Mäkinen, Zannini, Koehler, & Arendt, 2016; Ruiz et al., 2016a; Shen, Tang, & Li, 2021; Yang et al., 2022), the lower molecular weight peak and the shoulder can be assigned to the acidic and basic chains of globulin 11S, respectively. The higher molecular weight peak corresponds to the $8.6 \times 10^4$ g/mol fraction of MD of DE 7 that is present in the MD stock solution prior to phase separation (Fig. 3a). The chromatogram for the bottom phase for QPI-MD DE 2 mixture (Fig. 3d), which consisted of 20.7 % QPI and 4 % MD DE 2, shows a large peak at $2.6 \times 10^5$ g/mol followed by a shoulder at $5.5 \times 10^5$ g/mol. The peak corresponds to the main protein in QPI, globulin 11S, which is reported to have a molecular weight of 2.5 – 4.0 $\times 10^5$ g/mol (300 – 390 kDa) (Mir, Riar, & Singh, 2018; Ruiz et al, 2016a). The shoulder corresponds to the $5.0 \times 10^5$ g/mol fraction of MD DE 2 that is present in the MD stock solution prior to phase separation (Fig. 3b). Hence, the peaks representing higher $M_w$ in the chromatograms for both MDs (Fig. 3a-b) were also present in the data for each of the bottom phases (Fig. 3c-d). The smaller $M_w$ peaks, however, were absent, suggesting that the lower $M_w$ fractions preferentially partitioned into the top phases (Loret et al., 2005).

An atypical phase behaviour has previously been reported for mixtures of unrefined pea protein (PP) and sodium alginate (SA) (Mession et al., 2012a; Mession et al., 2012b). While the authors have manually fitted a binodal, the tie-lines of the PP-SA phase diagram indicate a shift of the binodal away from the axes. SA was reported to be entrapped in the highly viscous protein-rich bottom phase at increasing biopolymer concentration and at increasing fraction of SA in the starting mixture. Other mixtures, such as κ-carrageenan-soy protein (Li et al., 2008a), amylopectin-milk protein (de Bont, van Kempen, & Vreeker, 2002) and hydroxyethyl cellulose-latex colloids (Sperry, 1984) have displayed similar behaviour. Although latex particles and globular proteins are chemically and structurally different, they are both colloids and some of Sperry's (1984) elaborations are worth considering. Sperry (1984) observed that with increasing initial polysaccharide concentration and constant latex particle fraction in the system, the physical height of the latex particle-rich (bottom) phase increased. The height increase was proposed to be due to the formation of a volume-spanning network of latex particles with increasing interparticle void volume filled with

dissolved polysaccharide. An increase in the bottom phase height with increasing initial polysaccharide concentration (at constant protein concentration), indicating the possible formation of a volume-spanning network such as the one proposed by Sperry (1984), was also noted here for both QPI-MD systems (Supplementary material – B), and has been reported for other biopolymer mixtures involving proteins (de Bont et al., 2002; Li et al., 2008a; Mession et al., 2012b). Moreover, the tie-lines in the experimentally determined phase diagrams (Fig. 2) are not parallel, and the critical and threshold points do not coincide in either system, demonstrating asymmetry of the phase diagrams. According to Tolstoguzov (2000a), self-association of macromolecules can influence the excluded volume of the polymers and the affinity of the biopolymer molecules for the solvent, leading to a change in the slope of the tie-lines with an increase in the concentration of total biopolymer. Thus, the change in STL observed here could be explained by protein association and consequent entrapment of MD in the QPI-MD systems.

Before introducing micrographs acquired on the phase separated systems to elucidate their microstructure, it should be noted that the QPI stock solution contained protein aggregates (Supplementary material – C). Plant proteins are seldomly fully soluble in aqueous media, with a tendency to self-aggregation and high sedimentation rates, which is due to their complex quaternary structure and modifications in their physicochemical properties, caused by extraction and drying processes (Amagliani & Schmitt, 2017; Sarkar & Dickinson, 2020). Imaging the MD stock solutions by optical microscopy (1 mm – 0.2 μm) revealed no structures, confirming complete dissolution of both MDs.

The microstructure of samples collected along a tie-line for each phase-separated QPI-MD system is depicted in Fig. 4. The image labels correspond to the observed mixtures represented by the upper-case letters in Fig. 2. The images are a true representation of the whole sample that was viewed under the microscope. The middle column relates to the initial mixtures, both of which were prepared to lie at the centre of the tie-line and imaged immediately after preparation. The left-hand side column shows the top phases and the right-hand side column the bottom phases. The bright structures represent clusters of protein (Chen, Fang, Federici, Campanella, & Jones, 2020), as confirmed by the micrograph under the same conditions of the QPI stock solution alone (Supplementary material – C), while the MD stock solution appear as a dark background (not shown).

The microstructure of the top phases of the segregated mixtures (Fig. 4a and d) appear as protein aggregates varying in size from ~ 1–10 μm dispersed in a liquid continuous phase. The liquid phase is most likely pure MD, but the absence of soluble protein cannot be excluded. A similar microstructure was reported for the top/polysaccharide-rich phase of a sodium alginate-pea protein system (Mession et al., 2012b). Fig. 4b and e show the initial mixtures but the typical bicontinuous structure of phase separating biopolymer mixtures with equal phase volumes, usually at the centre point of a tie-line (Esquena, 2016), was not observed here in either system. Instead, the microstructure of the initial mixture is not unlike the microstructure of the top phases but denser in protein aggregates. The micrographs taken on the bottom phases of the segregated systems (Fig. 4c and f) show a percolated protein network structure with an entrapped liquid phase, which is likely close to pure MD but could also contain soluble protein. Considering the molecular weight data, it is reasonable to postulate that fractions of either MD are entrapped within this network, as suggested by Sperry (1984).

Collectively, the phase diagrams, the $M_w$ distribution of both MDs and the micrographs show that the QPI-MD systems display segregative phase behaviour, where the segregation mechanism is depletion flocculation. This mechanism has been reported to occur in mixtures involving globular proteins and polysaccharides (Ercelebi & Ibanoğlu, 2007; Gaaloul, Turgeon, & Corredig, 2009; Kim et al., 2006; Li, Deng, Hua, Qiu, Yang, & Cui, 2008b; Li et al., 2008a) with a phase separation threshold of less than 1.0 % (Doublier, Garnier, Renard, & Sanchez, 2000). Polysaccharide molecules lose conformational entropy when confined between two neighbouring globular molecules, giving rise to a region depleted of polymers. In the depleted region, the concentration of polymer is lower than in the bulk solution and a difference in osmotic pressure is created, which favours the displacement of solvent from the depleted region to the bulk. The difference in osmotic pressure induces attraction interactions between globular molecules (McClements, 2000; Tuinier, Dhont, & de Kruif, 2000). The phase separation threshold values determined from the experimental phase diagrams were 0.3 % and 1.2 % for MD of DE 7 and DE 2, respectively (Fig. 2), which is the first indication of depletion flocculation as the mechanism of phase separation (Doublier et al., 2000). Moreover, the shift of the binodals away from the axes (Fig. 2) and the increase in the bottom phase height with increasing MD concentration (Figure B.1) indicate that the self-association of QPI protein molecules during assumed depletion

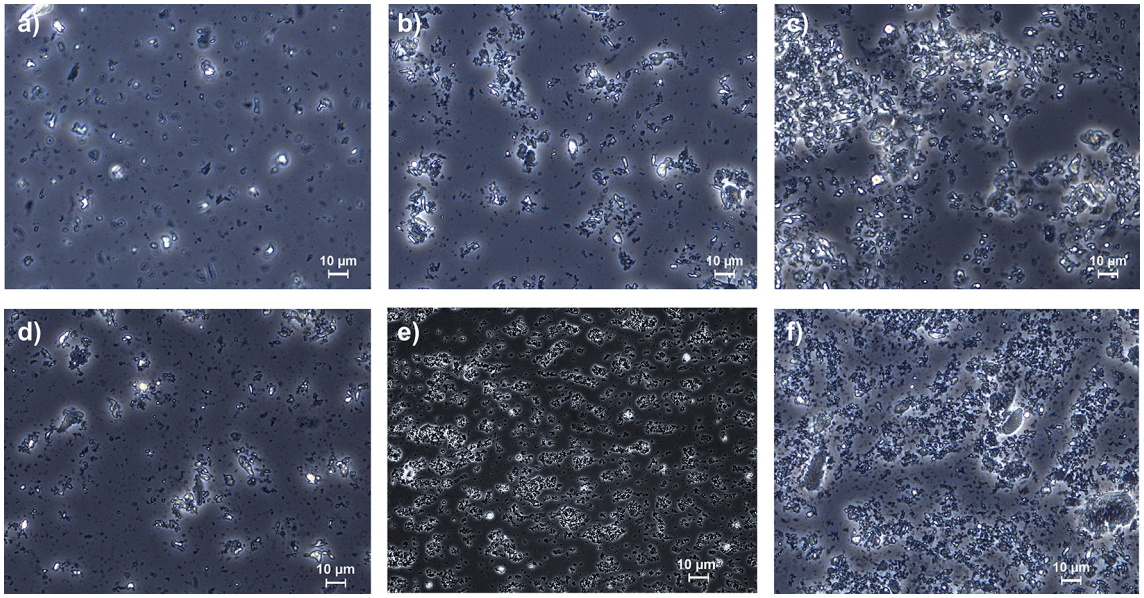


**Fig. 4.** Light microscopy images of QPI-MD mixtures. The top row relates to QPI-MD DE 7 and the tie-line indicated in Fig. 2a. The bottom row relates to the tie-line marked up in Fig. 2b for QPI-MD DE 2. From left to right, the columns relate to the top phase, initial mixture, and bottom phase. The image labels a)-f) concur with the upper-case letters A-F in Fig. 2. The bright structures identify protein and the scale bars are 10 μm.

flocculation behaviour led to the formation of a volume-spanning protein network, depicted in Fig. 4c and f, where the void volume was probably occupied by dissolved MD. The combination of depletion flocculation and the polysaccharide entrapment effect was also reported for κ-carrageenan-soy protein (Li et al., 2008a) and amylopectin-milk protein (de Bont et al., 2002) systems.

### 3.3. Effect of heat treatment and absence of salt on phase behaviour

The phase separation behaviour of biopolymer mixtures with a protein component is affected by protein conformation. Pre-heating a protein solution before mixing with a phase separating polysaccharide was previously reported to result in classical segregative phase separation behaviour (Chun et al., 2014; Kim et al., 2006). Since the native QPI-MD mixtures displayed an atypical phase behaviour, the influence of protein heat pre-treatment on one of the phase diagrams was examined.

The denaturation temperature of QPI was assessed by DSC (Fig. 5). A single endothermic peak with an onset temperature of 84.5 °C and peak temperature of 90.1 °C was obtained. The peak temperature is usually taken as the denaturation temperature ($T_d$) and the value found for the QPI extracted here is consistent for globulin 11S (chenopodin), the main protein in quinoa seeds (Vera, Valenzuela, Yazdani-Pedram, Tapia, & Abugoch, 2019). The presence of a single endothermic peak indicates either the predominance of globulin 11S or the presence of several proteins of similar thermostability (Ruiz et al., 2016a). Similar $T_d$ values have been reported for other plant globulins, such as pea protein ($T_d$ = 87.4 °C) (Mession et al., 2012a) and red bean protein ($T_d$ = 86 °C) (Meng & Ma, 2001).

Previously the response of almond proteins to thermal incubation has been used to select temperatures that induce limited protein denaturation, preventing gelation that can occur with a greater extent of unfolding. Hydrophobicity, circular dichroism and SDS-PAGE analyses were used to show that heat treatment of almond protein at moderate temperature (55 – 75 °C) induced partial protein denaturation and aggregation, while the use of high temperature (85 – 95 °C) led to gelation (Devnani, Ong, Kentish, & Gras, 2020). Additionally, a thermogram revealed a denaturation temperature of 81 °C for almond protein isolate, while no change in heat flow was observed at temperatures lower than the onset of 70 °C (Devnani, Ong, Kentish, & Gras, 2021). Based on these reports and the thermogram of QPI (Fig. 5), a temperature of 55 °C was selected for the pre-heating of QPI to produce heat treated QPI (HTQPI).

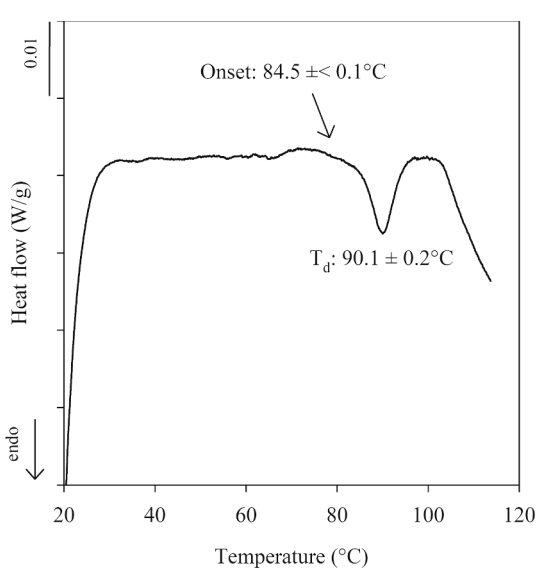


**Fig. 5.** Thermogram of QPI (10 %, w/w), showing only the heating step at a rate of 2 °C/min.

The resulting phase diagram, acquired with MD DE 2, is shown in Fig. 6a. The data is compared with the binodal for the original QPI-MD of DE 2 system. Consistent with Tolstoguzov (2002) reporting on biopolymer mixtures in general and Li et al. (2008a) discussing κ-carrageenan-soy protein mixtures, the thermal treatment of QPI decreased the phase separation threshold from 1.2 %, observed for the QPI-MD of DE 2 system, to 0.6 %. Nevertheless, the two-phase region was smaller in comparison to the original QPI-MD DE 2 system (black dashed line in Fig. 6a), evidencing that the heat treatment of QPI shifted the binodals further away from the axes as each biopolymer concentration is increased. On the other hand, the symmetry of the phase diagram increased for the heat-treated system, as demonstrated by the proximity of the critical and threshold points (Zaslavsky, 1995).

Micrographs taken of samples from the tie-line indicated in Fig. 6a and reproduced in Fig. 6b-d reveal similar microstructures, i.e., protein aggregation, as observed for the original QPI-MD system (Fig. 4). Evidently, the pre-heating of QPI did not yield the effect observed for whey protein isolate (WPI)-polysaccharide systems (Chun et al., 2014; Kim et al., 2006), i.e. a classical segregative phase separation. A major reason might be that in both studies, WPI was pre-heated at > 80 °C, i.e., above its thermal denaturation temperature and in the absence of salt.

As above-mentioned, another factor that can influence phase separation in aqueous media is the presence or absence of salt. At high concentrations, salt can partially shield the electrostatic repulsion between protein molecules, favouring hydrophobic interaction leading to increased association of protein molecules in biopolymer mixtures and greater incompatibility between proteins and polysaccharides (Grinberg & Tolstoguzov, 1997). Conversely, greater biopolymer compatibility may be expected at low salt concentrations, although salt can also influence solubility, making interactions complex.

Salt had a noticeable influence on the phase behaviour of the QPI-MD mixtures. Light micrographs of QPI-MD initial mixtures in the absence of salt (Supplementary material – D), captured immediately after mixture preparation, show a lower level of initial protein aggregation (Fig. D.1a and b, bright structures) than the observed in the original mixtures in the presence of NaCl (Fig. 4b and e). This observation is consistent with the literature for the influence of salt on protein molecules (Li, Cheng, Yi, Hua, Yang, & Cui, 2009). In contrast, the initial mixture of heat pre-treated QPI-MD DE 2 showed similar initial protein self-association when mixed in either the absence (Fig. D.1c) or presence of salt (Fig. 6c).

In the absence of salt, phase separation resulted in bottom phases of lower volume fractions than in the presence 0.1 M NaCl, indicating that QPI formed more compact bottom phases (Fig. 7). This suggests that the absence of salt had a larger impact on the QPI-rich phase, which is expected since QPI is the charged biopolymer in the systems. Still, the composition of the equilibrium phases points to a similar binodal shape to that displayed by QPI-MD mixtures in 0.1 M NaCl. In both cases the concentration of MD in the QPI-rich phase and of QPI in the MD-rich phase increased with overall biopolymer concentration. Similar phase behaviour in the absence of salt was observed for WPI in mixture with either κ-carrageenan or pectin (Chun et al., 2014) and for konjac glucomannan-milk mixtures (Dai, Jiang, Shah, & Corke, 2017). The data also indicate that MD fractionated between the phases in the mixtures without NaCl, illustrating that many aspects of segregative separation behaviour were common between samples with and without salt.

## 4. Conclusions

Systems involving quinoa protein isolate and maltodextrin of DE 7 and 2 are concluded to phase separate by depletion flocculation. The comparison between mathematically approximated and experimentally determined phase diagrams showed that QPI-MD mixtures followed a segregative separation behaviour but the shape of the binodals was atypical. As the initial biopolymer concentration increased, the polysaccharide and protein concentrations also increased in the QPI- and MD-rich phases, respectively, resulting in binodals that were shifted

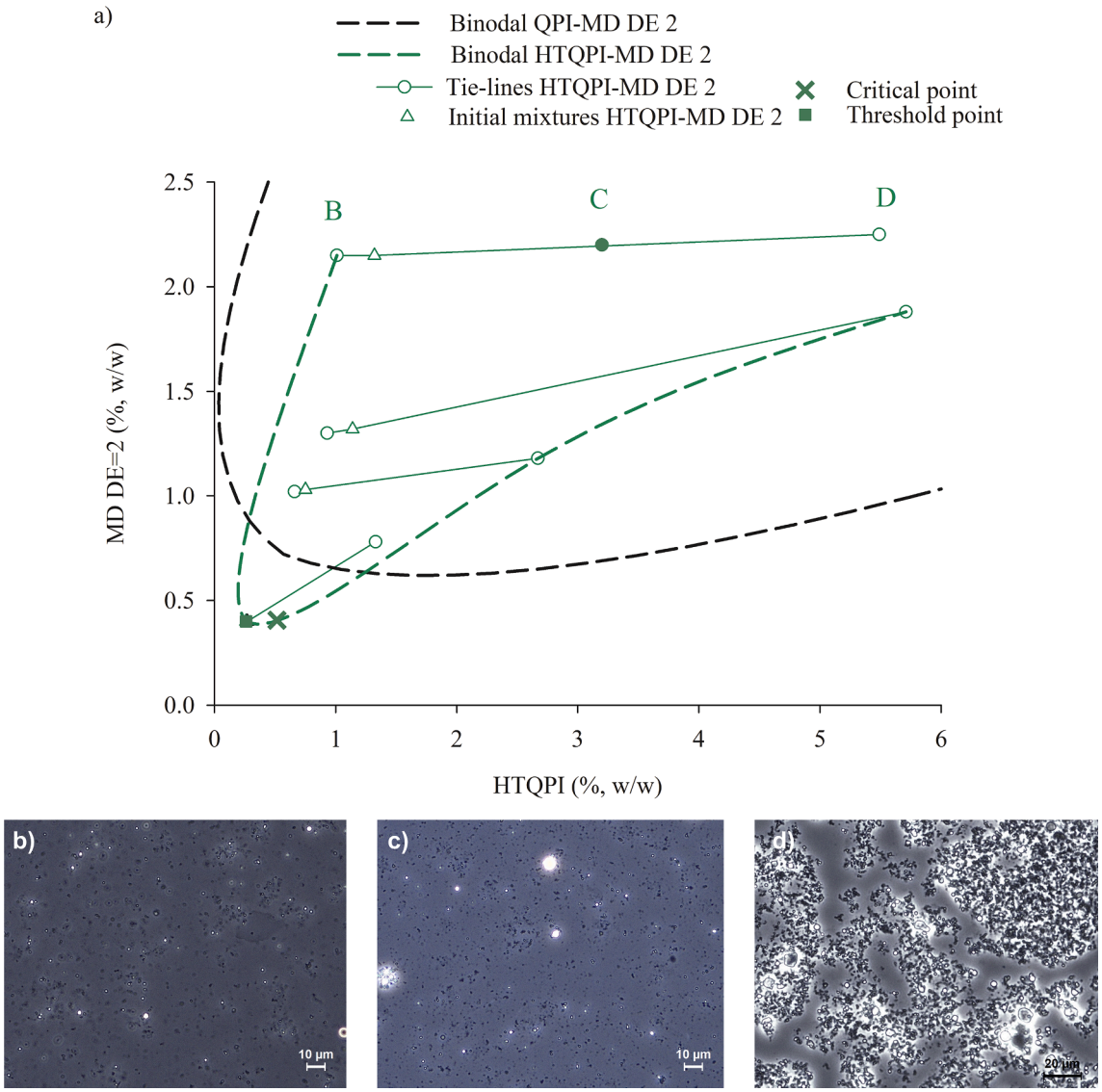


**Fig. 6.** Effect of heat pre-treatment on the phase behaviour of QPI-MD DE 2: a) experimental phase diagram between HTQPI and MD of DE 2 at pH 7.0, 22 °C and 0.1 M NaCl, the letters (B-D) identify the samples for which the microstructure was also analysed; b) top phase, c) initial mixture, and d) bottom phase. The bright structures are protein and the scale bars are 10 µm and 20 µm in length.

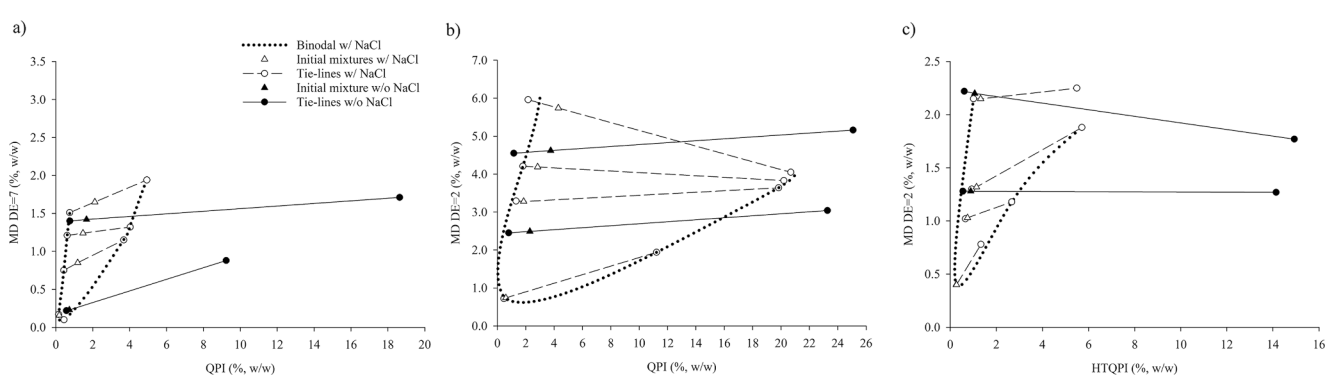


**Fig. 7.** Effect of the absence of NaCl on the phase behaviour of mixtures between a) QPI-MD MD 7; b) QPI-MD DE 2; and C) HTQPI-MD DE 2 at pH 7.0 and 22 °C.

away from the axes. *SEC*-MALS and microstructure analyses suggested that the phase compositions were affected by the fractionation of MD between the phases, and consequent entrapment of MD fractions within the aggregated network of the protein-rich phase. Similar atypical phase diagrams were observed when the systems were prepared in the absence of salt or when QPI was pre-heated before mixture with MD. The effect of pH on the phase behaviour of QPI-MD should be considered in future work. The results of this study are further evidence of the complicated

phase behaviour of *plant* proteins and polysaccharide mixtures. Thus, the formulation of products with predictable properties, that meet the current consumer demand for plant-based foods, may be challenging.

## CRediT authorship contribution statement

**Marina Campos Assumpção de Amarante:** Conceptualization, Formal analysis, Investigation, Methodology, Software, Validation, Visualization, Writing – original draft, Writing – review & editing. **Thomas MacCalman:** Methodology, Investigation. **Stephen E. Harding:** Methodology. **Fotis Spyropoulos:** Supervision, Writing – review & editing. **Sally Gras:** Conceptualization, Funding acquisition, Project administration, Resources, Supervision, Writing – review & editing. **Bettina Wolf:** Conceptualization, Funding acquisition, Project administration, Resources, Supervision, Writing – review & editing.

## Declaration of Competing Interest

The authors declare that they have no known competing financial interests or personal relationships that could have appeared to influence the work reported in this paper.

## Data availability

Data will be made available on request.

## Acknowledgement

This work was supported by the Priestley Joint PhD Scholarship from the University of Birmingham (UK) and The University of Melbourne (Australia).

## Appendix A. Supplementary material

Supplementary data to this article can be found online at https://doi.org/10.1016/j.foodres.2022.112064.

## References

Abugoch, L. E., Romero, N., Tapia, C. A., Silva, J., & Rivera, M. (2008). Study of some physicochemical and functional properties of quinoa (*Chenopodium Quinoa* Willd) protein isolates. *Journal of Agricultural and Food Chemistry, 56*(12), 4745–4750. https://doi.org/10.1021/jf703689u

Albalasmeh, A. A., Berhe, A. A., & Ghezzehei, T. A. (2013). A new method for rapid determination of carbohydrate and total carbon concentrations using UV spectrophotometry. *Carbohydrate Polymers, 97*(2), 253–261. https://doi.org/10.1016/j.carbpol.2013.04.072

Amagliani, L., & Schmitt, C. (2017). Globular plant protein aggregates for stabilization of food foams and emulsions. *Trends in Food Science and Technology, 67*, 248–259. https://doi.org/10.1016/j.tifs.2017.07.013

Antonov, Y. A., Dmitrochenko, A. P., & Leontiev, A. L. (2006). Interactions and compatibility of 11 S globulin from Vicia Faba seeds and sodium salt of carboxymethylcellulose in an aqueous medium. *International Journal of Biological Macromolecules, 38*(1), 18–24. https://doi.org/10.1016/j.ijbiomac.2005.12.011

Antonov, Y. A., Lashko, N. P., Glotova, Y. K., Malovikova, A., & Markovich, O. (1996). Effect of the structural features of pectins and alginates on their thermodynamic compatibility with gelatin in aqueous media. *Food Hydrocolloids, 10*(1), 1–9. https://doi.org/10.1016/S0268-005X(96)80047-6

Antonov, Y. A., Losinskaya, N. V., Grinberg, V. Y., Dianova, V. T., & Tolstoguzow, V. B. (1979). Phase equilibria in water-protein-polysaccharide systems. III. Water-soy bean globulins-polysaccharide systems. *Colloid and Polymer Science, 257*(11), 1159–1171. https://doi.org/10.1007/BF01517240

Antonov, Y. A., & Soshinsky, A. A. (2000). Interactions and compatibility of ribuloso-1,5-bisphosphate carboxylase/oxygenase from alfalfa with pectin in aqueous medium. *International Journal of Biological Macromolecules, 27*(4), 279–285. https://doi.org/10.1016/S0141-8130(00)00129-X

Antonov, Y. A., & Wolf, B. A. (2006). Phase behavior of aqueous solutions of bovine serum albumin in the presence of dextran, at rest, and under shear. *Biomacromolecules, 7*(5), 1562–1567. https://doi.org/10.1021/bm050899i

AOAC. (2002). *Official methods of analysis* (17th ed.). Association of Official Analytical Chemists.

Beldengrün, Y., Aragon, J., Prazeres, S. F., Montalvo, G., Miras, J., & Esquena, J. (2018). Gelatin/Maltodextrin Water-in-Water (W/W) Emulsions for the Preparation of Cross-Linked Enzyme-Loaded Microgels. *Langmuir, 34*(33), 9731–9743. https://doi.org/10.1021/acs.langmuir.8b01599

Cerdán-Leal, M. A., López-Alarcón, C. A., Ortiz-Basurto, R. I., Luna-Solano, G., & Jiménez-Fernández, M. (2020). Influence of heat denaturation and freezing–lyophilization on physicochemical and functional properties of quinoa protein isolate. *Cereal Chemistry, 97*(2), 373–381. https://doi.org/10.1002/cche.10253

Chen, D., Fang, F., Federici, E., Campanella, O., & Jones, O. G. (2020). Rheology, microstructure and phase behavior of potato starch-protein fibril mixed gel. *Carbohydrate Polymers, 239*(January). https://doi.org/10.1016/j.carbpol.2020.116247

Chronakis, I. S. (1998). On the molecular characteristics, compositional properties, and structural-functional mechanisms of maltodextrins: A review. *Critical Reviews in Food Science and Nutrition, 38*(7), 599–637. https://doi.org/10.1080/10408699891274327

Chun, J. Y., Hong, G. P., Surassmo, S., Weiss, J., Min, S. G., & Choi, M. J. (2014). Study of the phase separation behaviour of native or preheated WPI with polysaccharides. *Polymer, 55*(16), 4379–4384. https://doi.org/10.1016/j.polymer.2014.06.082

Dai, S., Jiang, F., Shah, N. P., & Corke, H. (2017). Stability and phase behavior of konjac glucomannan-milk systems. *Food Hydrocolloids, 73*, 30–40. https://doi.org/10.1016/j.foodhyd.2017.06.025

de Bont, P. W., van Kempen, G. M. P., & Vreeker, R. (2002). Phase separation in milk protein and amylopectin mixtures. *Food Hydrocolloids, 16*(2), 127–138. https://doi.org/10.1016/S0268-005X(01)00070-4

Devnani, B., Ong, L., Kentish, S., & Gras, S. (2020). Heat induced denaturation, aggregation and gelation of almond proteins in skim and full fat almond milk. *Food Chemistry, 325*, Article 126901. https://doi.org/10.1016/j.foodchem.2020.126901

Devnani, B., Ong, L., Kentish, S., & Gras, S. L. (2021). Structure and functionality of almond proteins as a function of pH. *Food Structure, 30*, Article 100229. https://doi.org/10.1016/j.foostr.2021.100229

Dickinson, E. (2019). Particle-based stabilization of water-in-water emulsions containing mixed biopolymers. *Trends in Food Science and Technology, 83*, 31–40. https://doi.org/10.1016/j.tifs.2018.11.004

Doublier, J.-L., Garnier, C., Renard, D., & Sanchez, C. (2000). Protein-polysaccharide interactions. *Current Opinion in Colloid and Interface Science, 5*, 171–198. https://doi.org/10.1201/9780203755617

Edelman, M. W., Tromp, R. H., & van der Linden, E. (2003). Phase-separation-induced fractionation in molar mass in aqueous mixtures of gelatin and dextran. *Physical Review E, 67*(2), Article 021404. https://doi.org/10.1103/PhysRevE.67.021404

Edelman, M. W., van der Linden, E., & Tromp, R. H. (2003). Phase Separation of Aqueous Mixtures of Poly(ethylene oxide) and Dextran. *Macromolecules, 36*(20), 7783–7790. https://doi.org/10.1021/ma0341622

Elsohaimy, S. A., Refaay, T. M., & Zaytoun, M. A. M. (2015). Physicochemical and functional properties of quinoa protein isolate. *Annals of Agricultural Sciences, 60*(2), 297–305. https://doi.org/10.1016/j.aoas.2015.10.007

Ercelebi, E. A., & Ibanoğlu, E. (2007). Influence of hydrocolloids on phase separation and emulsion properties of whey protein isolate. *Journal of Food Engineering, 80*(2), 454–459. https://doi.org/10.1016/j.jfoodeng.2006.05.027

Esquena, J. (2016). Water-in-water (W/W) emulsions. *Current Opinion in Colloid and Interface Science, 25*, 109–119. https://doi.org/10.1016/j.cocis.2016.09.010

Föste, M., Elgeti, D., Brunner, A. K., Jekle, M., & Becker, T. (2015). Isolation of quinoa protein by milling fractionation and solvent extraction. *Food and Bioproducts Processing, 96*, 20–26. https://doi.org/10.1016/j.fbp.2015.06.003

Frith, W. J. (2010). Mixed biopolymer aqueous solutions - Phase behaviour and rheology. *Advances in Colloid and Interface Science, 161*(1–2), 48–60. https://doi.org/10.1016/j.cis.2009.08.001

Gaaloul, S., Turgeon, S. L., & Corredig, M. (2009). Influence of shearing on the physical characteristics and rheological behaviour of an aqueous whey protein isolate-κappa-carrageenan mixture. *Food Hydrocolloids, 23*(5), 1243–1252. https://doi.org/10.1016/j.foodhyd.2008.09.011

Garnier, C., Schorsch, C., & Doublier, J. L. (1995). Phase separation in dextran/locust bean gum mixtures. *Carbohydrate Polymers, 28*(4), 313–317. https://doi.org/10.1016/0144-8617(95)00090-9

Geerts, M. E. J., Dekkers, B. L., van der Padt, A., & van der Goot, A. J. (2018). Aqueous fractionation processes of soy protein for fibrous structure formation. *Innovative Food Science and Emerging Technologies, 45*, 313–319. https://doi.org/10.1016/j.ifset.2017.12.002

Gharsallaoui, A., Yamauchi, K., Chambin, O., Cases, E., & Saurel, R. (2010). Effect of high methoxyl pectin on pea protein in aqueous solution and at oil/water interface. *Carbohydrate Polymers, 80*(3), 817–827. https://doi.org/10.1016/j.carbpol.2009.12.038

Grinberg, V. Y., & Tolstoguzov, V. B. (1997). Thermodynamic incompatibility of proteins and polysaccharides in solutions. *Food Hydrocolloids, 11*(2), 145–158. https://doi.org/10.1016/S0268-005X(97)80022-7

Guo, Q., Su, J., Yuan, F., Mao, L., & Gao, Y. (2019). Preparation, characterization and stability of pea protein isolate and propylene glycol alginate soluble complexes. *Lwt, 101*(November 2018), 476–482. https://doi.org/10.1016/j.lwt.2018.11.057

Horton, J. C., Harding, S. E., & Mitchell, J. R. (1991). Gel permeation chromatography-multi-angle laser light scattering characterization of the molecular mass distribution of 'Pronova' sodium alginate. *Biochemical Society Transactions, 19*(2), 510–511. https://doi.org/10.1042/bst0190510

Kasapis, S., Morris, E. R., Norton, I. T., & Clark, A. H. (1993). Phase equilibria and gelation in gelatin/maltodextrin systems - Part I: Gelation of individual components. *Carbohydrate Polymers, 21*(4), 243–248. https://doi.org/10.1016/0144-8617(93)90055-9

Kaspchak, E., de Oliveira, M. A. S., Simas, F. F., Franco, C. R. C., Silveira, J. L. M., Mafra, M. R., & Igarashi-Mafra, L. (2017). Determination of heat-set gelation capacity of a quinoa protein isolate (*Chenopodium quinoa*) by dynamic oscillatory rheological analysis. *Food Chemistry, 232*, 263–271. https://doi.org/10.1016/j.foodchem.2017.04.014

Kim, H.-J., Decker, E., & McClements, D. J. (2006). Preparation of multiple emulsions based on thermodynamic incompatibility of heat-denatured whey protein and pectin solutions. *Food Hydrocolloids, 20*(5), 586–595. https://doi.org/10.1016/j.foodhyd.2005.06.007

Klinjapo, R., & Krasaekoopt, W. (2018). Flavor in Confectionery Products. In *Natural and Artificial Flavoring Agents and Food Dyes*. Elsevier Inc. 10.1016/B978-0-12-811518-3/00014-4.

Lan, Y., Chen, B., & Rao, J. (2018). Pea protein isolate–high methoxyl pectin soluble complexes for improving pea protein functionality: Effect of pH, biopolymer ratio and concentrations. *Food Hydrocolloids, 80*, 245–253. https://doi.org/10.1016/j.foodhyd.2018.02.021

Lan, Y., Ohm, J.-B., Chen, B., & Rao, J. (2020a). Phase behavior, thermodynamic and microstructure of concentrated pea protein isolate-pectin mixture: Effect of pH, biopolymer ratio and pectin charge density. *Food Hydrocolloids, 101*, Article 105556. https://doi.org/10.1016/j.foodhyd.2019.105556

Lan, Y., Ohm, J. B., Chen, B., & Rao, J. (2020b). Phase behavior and complex coacervation of concentrated pea protein isolate-beet pectin solution. *Food Chemistry, 307*, Article 125536. https://doi.org/10.1016/j.foodchem.2019.125536

Li, X., Cheng, Y., Yi, C., Hua, Y., Yang, C., & Cui, S. (2009). Effect of ionic strength on the heat-induced soy protein aggregation and the phase separation of soy protein aggregate/dextran mixtures. *Food Hydrocolloids, 23*(3), 1015–1023. https://doi.org/10.1016/j.foodhyd.2008.07.024

Li, X., Deng, F., Hua, Y., Qiu, A., Yang, C., & Cui, S. (2008b). Effect of molecular weight of dextran on the phase behavior and microstructure of preheated soy protein/dextran mixtures. *Carbohydrate Polymers, 72*(1), 160–168. https://doi.org/10.1016/j.carbpol.2007.07.037

Li, X., Hua, Y., Qiu, A., Yang, C., & Cui, S. (2008a). Phase behavior and microstructure of preheated soy proteins and κ-carrageenan mixtures. *Food Hydrocolloids, 22*(5), 845–853. https://doi.org/10.1016/j.foodhyd.2007.04.008

Loret, C., Schumm, S., Pudney, P. D. A., Frith, W. J., & Fryer, P. J. (2005). Phase separation and molecular weight fractionation behaviour of maltodextrin/agarose mixtures. *Food Hydrocolloids, 19*(3), 557–565. https://doi.org/10.1016/j.foodhyd.2004.10.030

Mäkinen, O. E., Zannini, E., Koehler, P., & Arendt, E. K. (2016). Heat-denaturation and aggregation of quinoa (*Chenopodium quinoa*) globulins as affected by the pH value. *Food Chemistry, 196*, 17–24. https://doi.org/10.1016/j.foodchem.2015.08.069

Manoj, P., Kasapis, S., & Chronakis, I. S. (1996). Gelation and phase separation in maltodextrin-caseinate systems. *Food Hydrocolloids, 10*(4), 407–420. https://doi.org/10.1016/S0268-005X(96)80019-1

Mattice, K. D., & Marangoni, A. G. (2019). Comparing Methods to Produce Fibrous Material from Zein. *Food Research International, 128*, Article 108804. https://doi.org/10.1016/J.FOODRES.2019.108804

McClements, D. J. (2000). Comments on viscosity enhancement and depletion flocculation by polysaccharides. *Food Hydrocolloids, 14*(2), 173–177. https://doi.org/10.1016/S0268-005X(99)00065-X

Meng, G. T., & Ma, C. Y. (2001). Thermal properties of *Phaseolus angularis* (red bean) globulin. *Food Chemistry, 73*(4), 453–460. https://doi.org/10.1016/S0308-8146(00)00329-0

Mession, J. L., Assifaoui, A., Cayot, P., & Saurel, R. (2012a). Effect of pea proteins extraction and vicilin/legumin fractionation on the phase behavior in admixture with alginate. *Food Hydrocolloids, 29*(2), 335–346. https://doi.org/10.1016/j.foodhyd.2012.03.003

Mession, J. L., Assifaoui, A., Lafarge, C., Saurel, R., & Cayot, P. (2012b). Protein aggregation induced by phase separation in a pea proteins-sodium alginate-water ternary system. *Food Hydrocolloids, 28*(2), 333–343. https://doi.org/10.1016/j.foodhyd.2011.12.022

Mir, N. A., Riar, C. S., & Singh, S. (2019). Effect of pH and holding time on the characteristics of protein isolates from Chenopodium seeds and study of their amino acid profile and scoring. *Food Chemistry, 272*, 165–173. https://doi.org/10.1016/j.foodchem.2018.08.048

Mir, N. A., Riar, C. S., & Singh, S. (2018). Nutritional constituents of pseudo cereals and their potential use in food systems: A review. *Trends in Food Science and Technology, 75*, 170–180. https://doi.org/10.1016/j.tifs.2018.03.016

Murphy, K. M., Matanguihan, J. B., Fuentes, F. F., Gómez-Pando, L. R., Jellen, E. N., Maughan, P. J., & Jarvis, D. E. (2019). Quinoa Breeding and Genomics. In *Plant Breeding Reviews* (Vol. 42, pp. 257–320). 10.1002/9781119521358.ch7.

Nguyen, T. D., Lafarge, C., Murat, C., Mession, J., Cayot, N., & Saurel, R. (2014). Partition of volatile compounds in pea globulin–maltodextrin aqueous two-phase system. *Food Chemistry, 164*, 406–412. https://doi.org/10.1016/j.foodchem.2014.05.008

Nongonierma, A. B., Le Maux, S., Dubrulle, C., Barre, C., & FitzGerald, R. J. (2015). Quinoa (*Chenopodium quinoa* Willd.) protein hydrolysates with in vitro dipeptidyl peptidase IV (DPP-IV) inhibitory and antioxidant properties. *Journal of Cereal Science, 65*, 112–118. https://doi.org/10.1016/j.jcs.2015.07.004

Ruiz, G. A., Opazo-Navarrete, M., Meurs, M., Minor, M., Sala, G., van Boekel, M., … Janssen, A. E. M. (2016b). Denaturation and in Vitro Gastric Digestion of Heat-Treated Quinoa Protein Isolates Obtained at Various Extraction pH. *Food Biophysics, 11*(2), 184–197. https://doi.org/10.1007/s11483-016-9429-4

Ruiz, G. A., Xiao, W., van Boekel, M., Minor, M., & Stieger, M. (2016a). Effect of extraction pH on heat-induced aggregation, gelation and microstructure of protein isolate from quinoa (*Chenopodium quinoa* Willd). *Food Chemistry, 209*, 203–210. https://doi.org/10.1016/j.foodchem.2016.04.052

Saavedra-Leos, Z., Leyva-Porras, C., Araujo-Díaz, S. B., Toxqui-Terán, A., & Borrás-Enríquez, A. J. (2015). Technological application of maltodextrins according to the degree of polymerization. *Molecules, 20*(12), 21067–21081. https://doi.org/10.3390/molecules201219746

Sarbon, N. M., Badii, F., & Howell, N. K. (2015). The effect of chicken skin gelatin and whey protein interactions on rheological and thermal properties. *Food Hydrocolloids, 45*, 83–92. https://doi.org/10.1016/j.foodhyd.2014.10.008

Sarkar, A., & Dickinson, E. (2020). Sustainable food-grade Pickering emulsions stabilized by plant-based particles. *Current Opinion in Colloid and Interface Science, 49*, 69–81. https://doi.org/10.1016/j.cocis.2020.04.004

Shen, Y., Tang, X., & Li, Y. (2021). Drying methods affect physicochemical and functional properties of quinoa protein isolate. *Food Chemistry*, *339*(June 2020), 127823. 10.1016/j.foodchem.2020.127823.

Sperry, P. R. (1984). Morphology and mechanism in latex flocculated by volume restriction. *Journal of Colloid And Interface Science, 99*(1), 97–108. https://doi.org/10.1016/0021-9797(84)90089-4

Spyropoulos, F., Portsch, A., & Norton, I. T. (2010). Effect of sucrose on the phase and flow behaviour of polysaccharide/protein aqueous two-phase systems. *Food Hydrocolloids, 24*(2–3), 217–226. https://doi.org/10.1016/j.foodhyd.2009.09.008

Steffolani, M. E., Villacorta, P., Morales-Soriano, E. R., Repo-Carrasco, R., León, A. E., & Pérez, G. T. (2016). Physicochemical and functional characterization of protein isolated from different quinoa varieties (*Chenopodium quinoa* Willd.). *Cereal Chemistry Journal, 93*(3), 275–281. https://doi.org/10.1094/CCHEM-04-15-0083-R

Tolstoguzov, V. (2000a). Compositions and phase diagrams for aqueous systems based on proteins and polysaccharides. *International Review of Cytology, 192*.

Tolstoguzov, V. (2000b). Phase behaviour of macromolecular components in biological and food systems. *Nahrung - Food, 44*(5), 299–308. https://doi.org/10.1002/1521-3803(20001001)44:5<299::AID-FOOD299>3.0.CO;2-9

Tolstoguzov, V. (2002). Thermodynamic aspects of biopolymer functionality in biological systems, foods, and beverages. *Critical Reviews in Biotechnology, 22*(2), 89–174. https://doi.org/10.1080/07388550290789478

Tuinier, R., Dhont, J. K. G., & de Kruif, C. G. (2000). Depletion-Induced Phase Separation of Aggregated Whey Protein Colloids by an Exocellular Polysaccharide. *Langmuir, 16*(4), 1497–1507. https://doi.org/10.1021/la990202c

Vera, A., Valenzuela, M. A., Yazdani-Pedram, M., Tapia, C., & Abugoch, L. (2019). Conformational and physicochemical properties of quinoa proteins affected by different conditions of high-intensity ultrasound treatments. *Ultrasonics Sonochemistry, 51*, 186–196. https://doi.org/10.1016/j.ultsonch.2018.10.026

Vilcacundo, R., & Hernández-Ledesma, B. (2017). Nutritional and biological value of quinoa (*Chenopodium quinoa* Willd.). *Current Opinion in Food Science, 14*, 1–6. https://doi.org/10.1016/j.cofs.2016.11.007

Wang, Y. J., & Wang, L. (2000). Structures and Properties of Commercial Maltodextrins from Corn, Potato, and Rice Starches. *Starch/Staerke, 52*(7–8), 296–304. https://doi.org/10.1002/1521-379x(20009)52:8/9<296::aid-star296>3.0.co;2-a

WHO/FAO/UNU. (2007). Protein and amino acid requirements in human nutrition. *WHO Technical Report Series*, *935*.

Williams, M. A. K., Fabri, D., Hubbard, C. D., Lundin, L., Foster, T. J., Clark, A. H., … Hermansson, A. M. (2001). Kinetics of droplet growth in gelatin/maltodextrin mixtures following thermal quenching. *Langmuir, 17*(11), 3412–3418. https://doi.org/10.1021/la001811j

Yang, Z., de Campo, L., Gilbert, E. P., Knott, R., Cheng, L., Storer, B., … Hemar, Y. (2022). Effect of NaCl and CaCl2 concentration on the rheological and structural characteristics of thermally-induced quinoa protein gels. *Food Hydrocolloids, 124*, Article 107350. https://doi.org/10.1016/j.foodhyd.2021.107350

Zaslavsky, B. Y. (1995). *Aqueous two-phase partitioning; Physical chemistry and bioanalytical applications.* Marcel Dekker Inc.

Zheng, M., Jin, Z., & Zhang, Y. (2007). Effect of cross-linking and esterification on hygroscopicity and surface activity of cassava maltodextrins. *Food Chemistry, 103*(4), 1375–1379. https://doi.org/10.1016/j.foodchem.2006.10.053